

Evidence of Altered Posteromedial Cortical fMRI Activity in Subjects at Risk for Alzheimer Disease

Maija Pihlajamäki, MD, PhD,*†‡ Kelly O'Keefe, BA,*‡ Lars Bertram, MD,§
Rudolph E. Tanzi, PhD,§ Bradford C. Dickerson, MD,§|| Deborah Blacker, MD, ScD,‡
Marilyn S. Albert, PhD,¶ and Reisa A. Sperling, MD, MMSc*‡||

Abstract: The posteromedial cortices and other regions of the “default network” are particularly vulnerable to the pathology of Alzheimer disease (AD). In this study, we performed functional magnetic resonance imaging (fMRI) to investigate whether the presence of apolipoprotein E (*APOE*) $\epsilon 4$ allele and degree of memory impairment were associated with the dysfunction of these brain regions. Seventy-five elderly subjects ranging from cognitively normal to mild AD, divided into $\epsilon 4$ carriers and noncarriers, underwent fMRI during a memory-encoding task. Across all subjects, posteromedial and ventral anterior cingulate cortices (key components of the default network) as well as right middle and inferior prefrontal regions demonstrated reduced task-induced deactivation in the $\epsilon 4$ carriers relative to noncarriers. Even among cognitively normal subjects, $\epsilon 4$ carriers demonstrated reduced posteromedial deactivation compared with the noncarriers in the same regions which demonstrated failure of deactivation in AD patients. Greater failure of posteromedial deactivation was related to worse memory performance (delayed recall) across all subjects and within the range of cognitively normal subjects. In summary, the posteromedial cortical fMRI response pattern is modulated both by the presence of *APOE* $\epsilon 4$ and episodic memory capability. Altered fMRI activity of the posteromedial areas of the brain default network may be an early indicator of risk for AD.

Key Words: Alzheimer disease, apolipoprotein E (*APOE*), cognitive aging, functional magnetic resonance imaging (fMRI), mild cognitive impairment (MCI), memory

(*Alzheimer Dis Assoc Disord* 2009;00:000–000)

The structure and function of the posteromedial association cortices has garnered increasing attention as a potential indicator of prodromal Alzheimer disease (AD). functional magnetic resonance imaging (fMRI) studies in AD patients, compared with healthy elderly, have demonstrated alterations in posteromedial cortical activity during

goal-directed task performance versus low-level baseline conditions—termed as impaired task-induced deactivation or default network activity.^{1–4} Functional connectivity between the posteromedial cortices and other brain regions such as the medial temporal lobe is reported to be impaired even in subjects with mild cognitive impairment (MCI).^{5,6} Some structural MRI studies, but not all, have reported gray matter atrophy within the posteromedial cortices in MCI, particularly in subjects who progressed to clinical AD compared with those who remained cognitively stable.^{7,8} Optimally, however, prodromal AD would be detected before prominent structural atrophy—for example using functional imaging methods—at a point when disease-modifying therapies still might be able to prevent the progression to clinical dementia.

The primary known genetic risk factor for sporadic AD is the $\epsilon 4$ allele of the apolipoprotein E (*APOE*) gene.^{9,10} Previous [¹⁸F]fluorodeoxyglucose positron emission tomography (PET) studies in cognitively normal $\epsilon 4$ carriers, compared with noncarriers, have reported hypometabolism in the posteromedial cortices,^{11,12} in brain areas similar to those demonstrating impaired fMRI task-induced deactivation^{1–4} and reduced glucose metabolism^{13–16} in AD patients relative to healthy elderly controls. The effect of $\epsilon 4$ on the relative task-induced increases and decreases in fMRI signal remains, however, to be investigated. As the earliest and most salient cognitive deficit in AD is the inability to form enduring episodic memories, investigation of alterations in fMRI activity during memory encoding is of particular interest in subjects at genetic risk for AD.

In this study, we investigated older individuals across a range from cognitively intact to mild AD, with fMRI during associative encoding of face-name pairs. Our goal was to determine whether dysfunction of the same brain regions, which differentiate AD patients from healthy elderly, would relate to the presence of *APOE* $\epsilon 4$ allele and demonstrate a significant relationship with episodic memory performance. We hypothesized that fMRI activity of the posteromedial cortical areas of the default network would be impaired even in healthy elderly individuals at genetic risk for AD, and that more impaired posteromedial activity would relate to increasing impairment of episodic memory.

METHODS

Subjects

Seventy-five older individuals participated in the study. All subjects provided informed written consent in accordance with the Declaration of Helsinki and with the Human Research Committee guidelines of the Massachusetts

Received for publication November 11, 2008; accepted March 5, 2009. From the *Memory Disorders Unit, Department of Neurology, Brigham and Women's Hospital, Harvard Medical School; Departments of †Psychiatry; §Neurology; ||Athinoula A. Martinos Center for Biomedical Imaging, Massachusetts General Hospital, Boston, MA; ¶Department of Neurology, Johns Hopkins University School of Medicine, Baltimore, MD; and †Unit of Neurology, Institute of Clinical Medicine, University of Kuopio, Kuopio, Finland.

Supported by Academy of Finland grants #108188 and #214050 (M.P.), NINDS K23-NS02189 (R.S.), NIA R01 AG027435 (R.S.), NIA PO1-AG04953 (D.B./M.A./R.S.), and NIA P50-AG00513421 (R.S.).

Reprints: Maija Pihlajamäki, MD, PhD, Unit of Neurology, Institute of Clinical Medicine, University of Kuopio, P.O. Box 1627, FIN-70211 Kuopio, Finland (e-mail: Maija.Pihlajamaki@uku.fi).

Copyright © 2009 by Lippincott Williams & Wilkins

General Hospital and Brigham and Women's Hospital (Boston, MA).

The subjects were classified on the basis of their Clinical Dementia Rating (CDR) scores¹⁷ (Table 1): healthy elderly with a CDR score of 0.0 (n = 30); cognitively mildly impaired subjects with CDR 0.5, not demented (n = 30); subjects with mild dementia severity in terms of CDR 1.0 who also met the National Institute of Neurological and Communicative Disorders and Stroke/Alzheimer's Disease and Related Disorders Association criteria¹⁸ for probable AD (n = 15). AD patients had either been off cholinesterase inhibitors for at least 30 days before scanning or had never taken these medications. Sixty-five of the participants (older controls: n = 30; MCI: n = 30; and AD: n = 5) were recruited from a longitudinal study examining preclinical predictors of AD, and underwent additional neuropsychologic testing. The remaining 10 subjects (AD: n = 10) were recruited from memory disorder clinics. A subset of these subjects have been previously reported in 1 study using anatomically defined regions of interest limited to the medial temporal lobe (n = 29)¹⁹ and in another study using independent component analysis (n = 52).²⁰

For the purposes of this study (to investigate the relationship between episodic memory performance and regional fMRI activity), age-adjusted and education-adjusted Z-scores for the Rey Auditory Verbal Learning Test (RAVLT) delayed recall measures were calculated based on a large group of normal older subjects in our community.²¹

APOE Genotyping

The *APOE* polymorphisms were genotyped by restriction fragment length analysis following polymerase chain reaction from ~10 ng of genomic DNA, as described previously.²²

Among the 75 subjects, there were 28 *APOE* ε4 allele carriers (37%) (Table 2). When dividing the CDR groups into subgroups on the basis of the ε4 status, there were 9 out of 30 CDR 0.0 ε4 carriers (30%), 10 out of 30 CDR 0.5 ε4 carriers (33%), and 9 out of 15 CDR 1.0 ε4 carriers (60%). In this sample, there were 2 ε4 homozygotes, 1 in the CDR 0.0 and 1 in the CDR 0.5 group.

fMRI Paradigm and Postscan Memory Test

The fMRI paradigm consisted of blocks of novel and repeated face-name pairs alternating with visual fixation.²³ For the fixation baseline, the participants were instructed to focus their attention on a white crosshair presented on the black background. For the novel and repeated activation conditions, they were instructed to try (1) to remember the name associated with each face, (2) to make a subjective decision regarding whether or not they thought the name that "fit" the face, and (3) to press the response button with their index or middle finger accordingly. Each of the 6 fMRI runs consisted of 3 different conditions: 2 novel blocks (7 face-name pairs per block, each shown for 5 s) and 2 repeated blocks (2 randomly alternating face-name pairs) of identical length, separated by 25 seconds periods of fixation. The duration of the novel and repeated blocks combined was 140 seconds, and the duration of the fixation was 115 seconds per each run. Visual stimuli were presented using MacStim 2.5 software (WhiteAnt Occasional Publishing, West Melbourne, Australia). Images were projected through a collimating lens onto a screen attached to the head coil. Responses were collected using a fiber-optic response box held in the right hand.

After the scanning session all subjects underwent a forced-choice associative recognition memory test. During this "name recognition" test, a set of 12 novel faces seen

TABLE 1. Characteristics of the Subject Groups

	CDR		
	CDR = 0.0 (n = 30)	CDR = 0.5 (n = 30)	CDR = 1.0 (n = 15)
Demographics			
Age, y	74.0 ± 5.5	76.7 ± 5.3	78.3 ± 6.9
(range)	(66-90)	(67-87)*	(57-85)*
Education, y	15.6 ± 2.6	15.8 ± 3.2	13.3 ± 3.2
(range)	(12-21)	(12-25)	(8-20)*†
Female/male; % of female	19/11; 63	19/11; 63	8/7; 53
Cognition			
CDR-SB	0.0 ± 0.0	1.8 ± 1.0	4.6 ± 0.7
(range)	(0.0-0.0)	(0.5-3.5)*	(3.5-6.0)*†
MMSE	29.6 ± 0.5	29.1 ± 1.1	23.3 ± 4.2
(range)	(29-30)	(26-30)*	(15-30)*†
RAVLT delayed recall	0.2 ± 0.8	-0.5 ± 1.4	-2.5 ± 1.0
(range)‡	(-0.8-2.0)	(-2.6-2.0)	(-3.9- -1.3)*†
GM volume			
GM volume × 10 ⁵ , mm ³	6.6 ± 0.5	6.5 ± 0.4	5.9 ± 0.4
(range)	(5.7-7.3)	(5.6-7.2)*	(5.1-6.6)*†
Postscan memory test			
Name recognition, %	87.3 ± 9.7	84.1 ± 13.0	65.7 ± 11.7
(range)	(64-100)	(43-100)*	(50-86)*†

Given are the means ± SDs.

Significant differences between groups ($P < 0.05$, Mann-Whitney U test and χ^2 test).

*Versus CDR = 0.0.

†Versus CDR = 0.5.

‡In the CDR = 1.0 group, RAVLT scores were available for 5 out of 15 subjects.

CDR indicates Clinical Dementia Rating; CDR-SB, CDR Sum-of-Box score; GM, gray matter; MMSE, Mini-Mental State Examination; RAVLT, Rey Auditory Verbal Learning Test.

TABLE 2. Characteristics of the APOE ε4 Noncarriers and Carriers Across All Subjects and Within Each Subgroup

	CDR							
	All Subjects (n = 75)		CDR = 0.0 (n = 30)		CDR = 0.5 (n = 30)		CDR = 1.0 (n = 15)	
	ε4- (n = 47)	ε4+ (n = 28)	ε4- (n = 21)	ε4+ (n = 9)	ε4- (n = 20)	ε4+ (n = 10)	ε4- (n = 6)	ε4+ (n = 9)
Demographics								
Age, y	75.9 ± 6.1	76.0 ± 5.6	74.8 ± 5.4	72.2 ± 5.8	76.8 ± 5.6	76.5 ± 4.7	77.0 ± 10.1	79.1 ± 4.3
(range)	(57-90)	(66-85)	(68-90)	(66-81)	(67-87)	(67-84)	(57-84)	(73-85)
Education, y	15.2 ± 2.7	15.2 ± 3.7	15.6 ± 2.5	15.5 ± 3.0	15.6 ± 2.7	16.2 ± 4.2	12.5 ± 2.3	13.9 ± 3.6
(range)	(9-20)	(8-25)	(12-19)	(12-21)	(12-20)	(12-25)	(9-16)	(8-20)
Female/male; % of female	27/20; 57	19/9; 68	11/10; 52	8/1; 89	13/7; 65	6/4; 60	3/3; 50	5/4; 55
Cognition								
CDR-SB	1.3 ± 1.8	2.2 ± 1.8	0.0 ± 0.0	0.0 ± 0.0	1.6 ± 1.0	2.5 ± 0.9	5.2 ± 0.4	4.2 ± 0.5
(range)	(0.0-6.0)	(0.0-5.0)	(0.0-0.0)	(0.0-0.0)	(0.5-3.5)	(1.5-3.5)*	(5.0-6.0)	(3.5-5.0)†
MMSE	28.6 ± 2.8	27.4 ± 3.5	29.6 ± 0.5	29.7 ± 0.5	29.2 ± 1.1	28.9 ± 1.1	23.2 ± 5.2	23.3 ± 3.7
(range)	(15-30)	(17-30)	(29-30)	(29-30)	(26-30)	(27-30)	(15-29)	(17-30)
RAVLT delayed recall	-0.4 ± 1.3	-0.3 ± 1.4	0.1 ± 0.7	0.5 ± 0.9	-0.5 ± 1.5	-0.5 ± 1.2	-2.3 ± 0.9	-2.8 ± 1.5
(range)‡	(-3.0-2.0)	(-3.9-2.0)	(-0.8-1.6)	(-0.7-2.0)	(-2.6-2.0)	(-2.2-2.0)	(-3.0-1.3)	(-3.9-1.7)
GM volume								
GM volume × 10 ⁵ , mm ³	6.5 ± 0.5	6.3 ± 0.5	6.6 ± 0.4	6.6 ± 0.6	6.6 ± 0.4	6.3 ± 0.4	5.9 ± 0.3	5.9 ± 0.4
(range)	(5.5-7.3)	(5.1-7.3)	(5.9-7.3)	(5.7-7.3)	(5.6-7.2)	(5.6-6.8)	(5.5-6.4)	(5.1-6.6)
Postscan memory test								
Name recognition, %	84.1 ± 11.4	77.6 ± 16.9	86.5 ± 9.9	89.0 ± 9.6	86.5 ± 8.7	79.4 ± 18.6	68.0 ± 12.8	64.2 ± 11.5
(range)	(50-100)	(43-100)	(64-100)	(71-100)	(71-100)	(43-100)	(50-79)	(50-86)

Given are the means ± SDs.

Significant differences between groups ($P < 0.05$, Mann-Whitney U test and χ^2 test).

*Versus CDR = 0.5 ε4-.

†Versus CDR = 1.0 ε4-.

‡In the CDR = 1.0 group, RAVLT scores were available for 3 out of 6 ε4 noncarriers and 2 out of 9 ε4 carriers.

CDR indicates Clinical Dementia Rating; CDR-SB, CDR sum-of-box score; GM, gray matter; MMSE, Mini-Mental State Examination; RAVLT, Rey Auditory Verbal Learning Test.

during the experiment and the 2 repeated faces were presented on a computer screen. Each face was shown with 2 names printed underneath: the correct name that was paired with the face during scanning and 1 incorrect name that was previously paired with a different face during scanning. The subjects were instructed to indicate the correct name by pointing to it on the computer monitor.

MRI Data Acquisition

Subjects were scanned using a Siemens Trio 3.0T scanner (Siemens Medical Systems, Iselin, NJ) equipped for echo-planar imaging. High-resolution structural images were acquired using a T₁-weighted 3 dimensional magnetization prepared rapid acquisition gradient echo sequence with the following parameters: repetition time = 2530 ms, echo time = 3.45 ms, inversion time = 1100 ms, flip angle = 7 degree, field of view = 256 mm, matrix 192 × 256, slice thickness = 1.33 mm, and 128 sagittal slices. Blood-oxygen-level-dependent (BOLD) fMRI data were scanned using a T₂*-weighted gradient-echo echo-planar imaging sequence: repetition time = 2500 ms, echo time = 30 ms, flip angle = 90 degree, field of view = 200 mm, and matrix 64 × 64 (in-plane resolution 3.125 × 3.125 mm²). Twenty-eight oblique coronal slices with a thickness of 5.0 mm and an interslice gap of 1.0 mm were acquired, oriented perpendicular to the anterior-posterior commissural line. Scanning time for each functional run was 4 minutes 15 seconds and consisted of 102 whole-brain acquisitions. Total functional scanning time of 6 fMRI runs was 25 minutes 30 seconds.

Demographic and Cognitive Data Analysis

Differences in age, education, and cognitive performance were tested using the nonparametric Mann-Whitney *U* test and differences in sex distribution using χ^2 test in SPSS 14.0 (SPSS Inc, Chicago, IL). The level of statistical significance was set at $P < 0.05$.

Structural MRI Data Analysis

Brain gray matter volume, normalized for head size, was estimated in a fully automated way with SIENAX, part of FSL.²⁴ Brain and skull images were first extracted from the single whole-head input data of each subject. Brain images were affine-registered to Montreal Neurological Institute (MNI) space (using the skull image to determine the registration scaling). Peripheral gray matter volumes were then calculated using tissue-type segmentation with partial volume estimation. Differences in gray matter volumes between groups were tested using the Mann-Whitney *U* test in SPSS 14.0 and considered statistically significant at $P < 0.05$.

fMRI Data Analysis

The goal of this study was to investigate alterations in fMRI activity in the default network and related association cortical areas. To this aim, active processing of novel face-name pairs was contrasted to the fixation baseline. Both increase and decrease in BOLD signal evoked during task performance were examined. fMRI data analysis was carried out using FEAT 5.63, part of FSL (www.fmrib.ox.ac.uk/fsl). The following prestatistical processing was applied: motion correction, removal of nonbrain structures, spatial smoothing using a Gaussian kernel of full width at half maximum of 5 mm, mean-based intensity normalization of all volumes by the same factor, and high-pass temporal filtering

with a frequency cut-off point of 140.0 seconds. Time-series statistical analysis was carried out using FILM with local autocorrelation correction. fMRI images were registered to high-resolution structural images and to the MNI standard brain using FLIRT and 12 parameter affine registration.

Higher-level between-group analyses were carried out using FLAME including age, sex, and gray matter volume as covariates.²⁵ FSL mixed-effects modeling exploits 2-sample unpaired *t* tests for between-group analyses. The resulting Z-statistic images (Gaussianised *T* statistic images) were corrected for multiple comparisons using cluster thresholding.²⁶ To perform cluster thresholding, default FSL values for the voxelwise Z-statistic threshold ($Z > 2.3$) and the cluster probability threshold ($P < 0.05$) were applied. Analyses between $\epsilon 4$ carriers and noncarriers were confined to regions affected in AD by using the whole-brain statistical map ($P < 0.05$, cluster-corrected) resulting from the comparison between healthy elderly (CDR = 0.0) and AD patients (CDR = 1.0) as a mask (Table 3, Figs. 1, 2).

The region-of-interest (ROI) analysis of BOLD signal magnitude was performed by positioning the center of a sphere 5 voxels in diameter into the peak MNI coordinates in the $\epsilon 4$ carriers versus noncarriers statistical maps. Mean BOLD signal change (in percentages) during processing novel face-name pairs versus fixation was extracted for each subject and region using FSL featquery and entered into SPSS for statistical analysis using the 1-way analysis of variance, 2-sample unpaired *t* tests and Pearson correlation. The ROI analyses were performed to complement the FSL group-level data analyses by investigating the directionality of the BOLD signal differences and also to provide some insight into the inter-individual variability of the fMRI response across the elderly subject groups. Of the results presented below, the correlations with the memory measures as well as the bar graphs and scatter plots presented in Figures 1 and 2 are based on the ROI analyses of fMRI signal response.

TABLE 3. Brain Areas Demonstrating Different fMRI Activity ($P < 0.05$, Cluster-Corrected) Between AD Patients (CDR = 1.0) and Healthy Elderly (CDR = 0.0) During Processing of Novel Face-name Pairs Compared With Fixation

Brain Region	Peak MNI Coordinate (x, y, z)	Peak Z-score
R precuneus, posterior cingulum	10, -68, 40	3.85
L precuneus, posterior cingulum	-6, -68, 34	3.54
L supramarginal gyrus	-36, -72, 34	3.29
R anterior cingulum (ventral)	8, 44, 12	4.09
R anterior cingulum (dorsal)	6, 20, 30	3.44
L anterior cingulum (dorsal)	0, 22, 38	3.00
R middle frontal gyrus	36, 32, 26	4.21
R inferior frontal gyrus, insular sulcus	38, 22, 8	3.71
L inferior frontal gyrus, insular sulcus	-36, 16, -16	4.34
R lingual gyrus	16, -64, 0	3.08
R occipital pole	10, -92, -22	3.70
L occipital pole	-4, -90, -14	3.38
L temporopolar cortex	-34, 10, -28	3.18
L hippocampus, rhinal cortex	-24, -6, -28	2.45

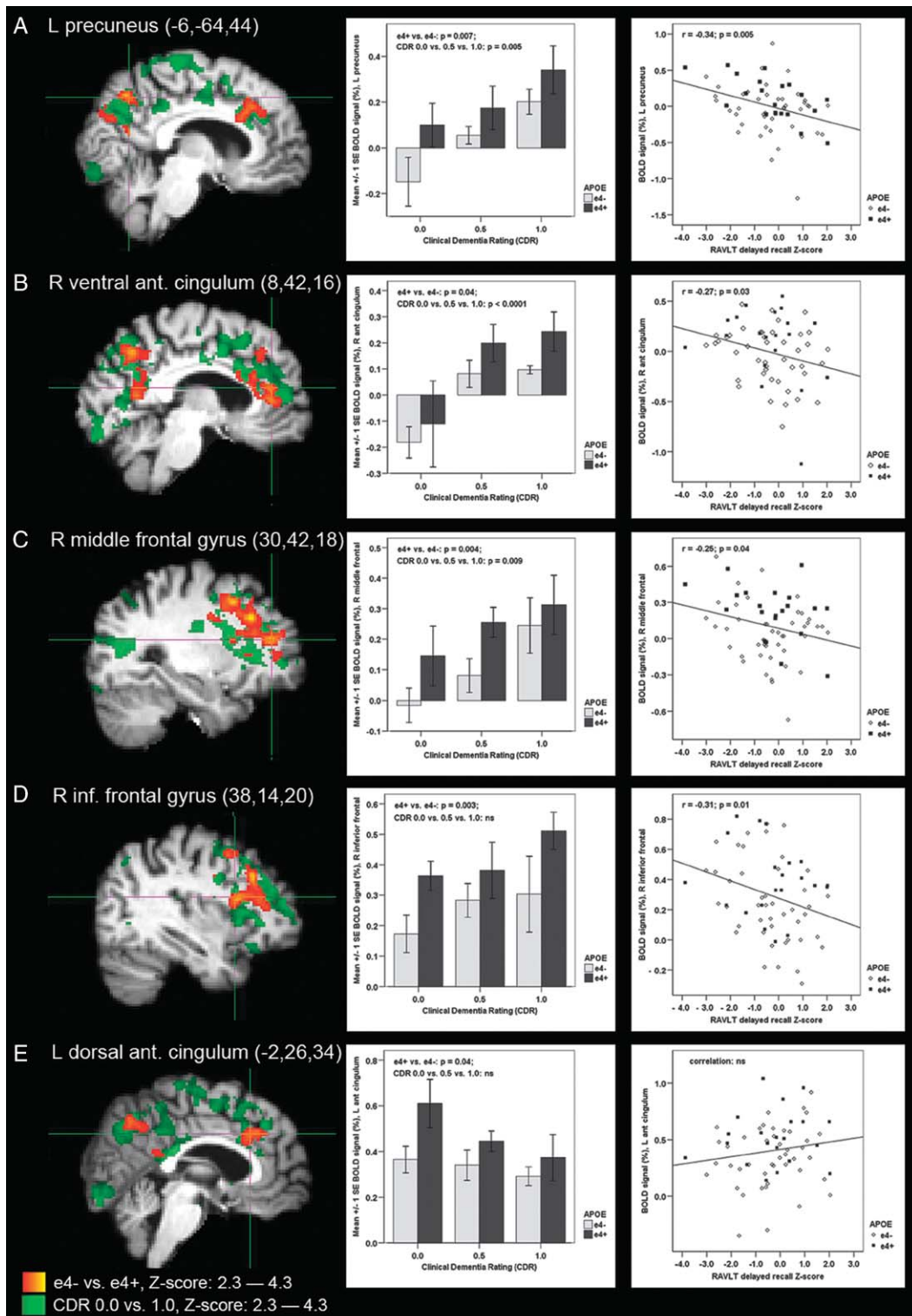
AD indicates Alzheimer disease; CDR, Clinical Dementia Rating; fMRI, functional magnetic resonance imaging; L, left; MNI, Montreal Neurological Institute; R, right.

RESULTS

Subject Characteristics

The 3 clinical groups (healthy elderly with CDR 0.0, mildly impaired subjects with CDR 0.5, and AD patients

with CDR 1.0) differed on several demographic and cognitive variables as indicated in Table 1. In contrast, there were no differences in demographic or cognitive characteristics between $\epsilon 4$ carriers and noncarriers either across all subjects or within each CDR group (Table 2), except that the



CDR 1.0 $\epsilon 4$ carriers had lower ($P = 0.002$) and the CDR 0.5 $\epsilon 4$ carriers higher ($P = 0.02$) CDR sum-of-boxes scores than the noncarriers.

Gray Matter Volumes

The mean gray matter volume was significantly smaller in AD patients than in the CDR 0.5 ($P = 0.001$, Mann-Whitney U test) and CDR 0.0 ($P < 0.0001$) subjects (Table 1). There were no differences in gray matter volumes between all $\epsilon 4$ carriers and noncarriers or between the $APOE$ groups within the CDR groups (Table 2).

fMRI—Areas of Altered Activity in AD Compared With Healthy Elderly

We first compared AD patients (CDR 1.0) with the healthy elderly (CDR 0.0) during the processing of novel face-name pairs compared with fixation. Significant differences in fMRI activity ($P < 0.05$, cluster-corrected) were found in: right and left precuneus and posterior cingulum, dorsal anterior cingulum, left supramarginal gyrus, and right ventral anterior cingulum; right middle frontal and right and left inferior frontal and insular cortices; right and left occipital pole, right lingual and left temporopolar cortices, left hippocampus, and the surrounding rhinal cortex (Table 3, Fig. 1). The whole-brain statistical map resulting from the AD versus healthy elderly between-group comparison comprising brain regions listed above was used as a mask to confine further data analyses to the areas affected in AD. As can be seen in Figure 1, among the brain regions affected both by AD and $APOE$ $\epsilon 4$ allele, all areas (Figs. 1A–D) except the dorsal anterior cingulate cortex (Fig. 1E) demonstrated greater positive BOLD fMRI signal in AD patients than in healthy elderly subjects.

fMRI—Effect of $APOE$ $\epsilon 4$ and Correlations With Memory Performance Across All Subjects

We then compared fMRI activity between $APOE$ $\epsilon 4$ carriers and noncarriers across all 75 subjects within the brain areas affected in AD as described above. The $\epsilon 4$ carriers and noncarriers demonstrated significantly different fMRI activity in: right precuneus (peak MNI coordinate: 8, -64, 44; corresponding Z -score = 3.49), left precuneus and posterior cingulum (MNI: -6, -64, 44; $Z = 3.61$), right ventral anterior cingulum (MNI: 8, 42, 16; $Z = 3.21$), left dorsal anterior cingulum (MNI: -2, 26, 34; $Z = 3.21$), right middle frontal (MNI: 30, 42, 18; $Z = 3.65$), and inferior frontal and insular cortices (MNI: 38, 14, 20; $Z = 3.65$) (Fig. 1).

ROI analysis revealed that in each of these regions fMRI signal was more positive (less task-induced deactivation or more activation) in the $\epsilon 4$ carriers than in

noncarriers (Fig. 1). In the precuneal and ventral anterior cingulate ROIs, we found the most negative BOLD signal (the greatest task-induced deactivation) in the healthy elderly $\epsilon 4$ noncarriers and the most positive BOLD signal (paradoxical activation) in the AD $\epsilon 4$ carriers.

In the 65 subjects with additional neuropsychologic testing, we further investigated whether regional BOLD signal magnitude correlated with RAVLT delayed recall performance. Four of the 6 regions which showed altered fMRI activity in $\epsilon 4$ carriers demonstrated significant inverse correlation with the RAVLT delayed recall scores: left precuneus ($r = -0.34$; $P = 0.005$), right ventral anterior cingulum ($r = -0.27$; $P = 0.03$), as well as right middle ($r = -0.25$; $P = 0.04$) and inferior ($r = -0.31$; $P = 0.01$) prefrontal cortices (Fig. 1). Similarly, we found the performance in the postscan recognition memory test to correlate significantly with the fMRI activity in the following brain regions: right ($r = -0.42$; $P < 0.001$) and left precuneus ($r = -0.31$; $P = 0.006$), right ventral anterior cingulum ($r = -0.35$; $P = 0.002$), and right inferior prefrontal cortex ($r = -0.33$; $P = 0.004$). Altogether, greater positive BOLD signal (less deactivation) was correlated with the worse episodic memory performance.

fMRI—Effect of $APOE$ $\epsilon 4$ and Correlations With Memory Performance Within Healthy Elderly

We then examined the effect of $\epsilon 4$ within the group of healthy elderly individuals (CDR 0.0). Significant differences in fMRI activity ($P < 0.05$, cluster-corrected) between the normal $\epsilon 4$ carriers and noncarriers were found in: right (MNI: 8, -62, 42; $Z = 3.28$) and left (MNI: -10, -68, 44; $Z = 3.09$) precuneus (Fig. 2). The ROI analysis demonstrated negative BOLD signal (preserved deactivation) in noncarriers, compared with positive BOLD signal (failure of deactivation) in the $\epsilon 4$ carriers, similar to the paradoxical activation observed in the AD patients. Greater positive BOLD signal (less deactivation) in the left precuneus was inversely correlated with RAVLT delayed recall scores ($r = -0.39$; $P = 0.03$) even within the healthy elderly, similar to the findings observed across all subjects. The correlation between postscan forced-choice recognition memory performance and regional fMRI activity did not reach statistical significance in the healthy older subjects only, perhaps due to the high performance on this relatively easy forced-choice recognition task in most of the healthy subjects.

DISCUSSION

This study provides evidence that the function of the posteromedial cortices is more impaired in carriers of the $APOE$ $\epsilon 4$ allele, compared with noncarriers, across a range

FIGURE 1. fMRI statistical maps of apolipoprotein E ($APOE$) $\epsilon 4$ carriers ($\epsilon 4+$) compared with noncarriers ($\epsilon 4-$) across all subjects, ranging from healthy elderly with CDR of 0.0 to patients with AD (CDR=1.0), demonstrated differential fMRI activity ($P < 0.05$, cluster-corrected) in: (A) L precuneus, (B) R ventral anterior cingulum, (C) R middle frontal gyrus, (D) R inferior frontal gyrus, and (E) L dorsal anterior cingulum (Montreal Neurological Institute coordinates of the crosshairs are reported in the figure). In each of these regions, magnitude of fMRI signal was greater in the $\epsilon 4$ carriers than in noncarriers (unpaired t test, 2-tailed uncorrected P values are indicated in the figure). Difference in BOLD signal magnitude across the CDR groups was tested using 1-way analysis of variance (P values reported in the figure). Scatter plots demonstrate the relationship between regional BOLD signal and Rey Auditory Verbal Learning (RAVLT) delayed recall scores (Pearson correlation, r and P values are indicated in the figure). The statistical map presenting significantly different activation areas in $\epsilon 4$ carriers versus noncarriers (red-yellow) is overlaid on the statistical map demonstrating significantly different activation areas in AD patients versus healthy elderly (dark green-light green). AD indicates Alzheimer disease; BOLD, blood-oxygen-level-dependent; CDR, Clinical Dementia Rating; fMRI, functional magnetic resonance imaging; L, left; NS, not significant; R, right.

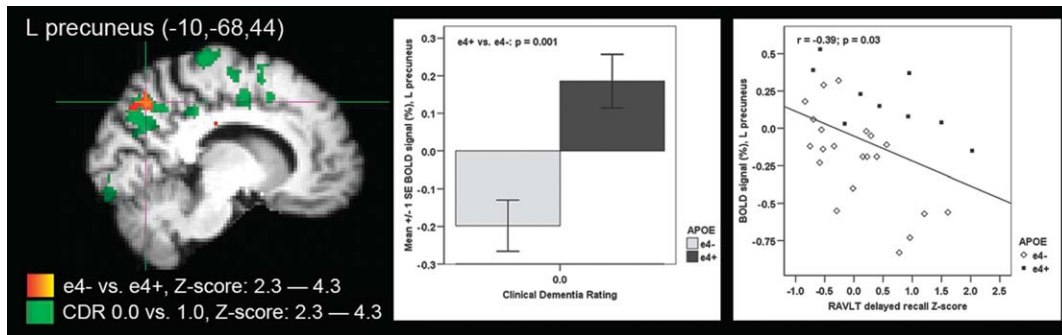


FIGURE 2. Within the group of healthy elderly with Clinical Dementia Rating (CDR) of 0.0, fMRI activity ($P < 0.05$, cluster-corrected) in the apolipoprotein E (*APOE*) $\epsilon 4$ carriers ($\epsilon 4+$) differed significantly from that of noncarriers ($\epsilon 4-$) in the left (L) precuneus. Region-of-interest analysis revealed greater BOLD fMRI signal magnitude in the $\epsilon 4$ carriers than in noncarriers ($P = 0.001$, unpaired t test). Greater positive BOLD signal (ie, reduced fMRI task-induced deactivation) was related to poorer Rey Auditory Verbal Learning (RAVLT) delayed recall performance ($P = 0.03$, Pearson correlation). The statistical map presenting significantly different activation areas in $\epsilon 4$ carriers versus noncarriers (red-yellow) is overlaid on the statistical map demonstrating significantly different activation areas in Alzheimer disease (AD) patients versus healthy elderly (dark green-light green). BOLD indicates blood-oxygen-level-dependent; fMRI, functional magnetic resonance imaging.

of cognitive ability. Failure of memory-related deactivation in these key regions of the default network was evident even among healthy elderly individuals who carry the *APOE* $\epsilon 4$ allele. Furthermore, magnitude of BOLD fMRI signal of the left posteromedial cortical region, which showed significant $\epsilon 4$ -related dysfunction, was related to verbal episodic memory performance, even within the range of cognitively normal older subjects. These findings suggest that fMRI activity in the posteromedial cortical areas of the default network is modulated by 2 major risk factors for AD, that is, the presence of *APOE* $\epsilon 4$ allele and incipient episodic memory impairment.

Previous studies have reported evidence of impaired fMRI deactivation in subjects with MCI compared with the healthy elderly^{3,4} and in $\epsilon 4$ carriers compared with the noncarriers.²⁷ This study investigated the entire continuum from cognitively intact subjects at genetic risk for AD to subjects with cognitive impairment (CDR 0.5) to those with clinical AD, and found that the $\epsilon 4$ allele was associated with more impaired activity of regions of the default network throughout the course of the disease. Furthermore, $\epsilon 4$ carriers without any clinical impairment demonstrated impaired fMRI activity in the same posteromedial cortical regions, which were found to differentiate AD patients from healthy older subjects.

Our finding of dysfunction of the posteromedial cortices in cognitively normal elderly individuals at genetic risk for AD is consistent with the previous fluorodeoxyglucose-PET results of abnormal resting-state metabolism in $\epsilon 4$ carriers versus noncarriers^{11,12} and a recent fMRI study.²⁷ Furthermore, molecular PET imaging using a tracer called [¹¹C]Pittsburgh Compound B, has recently provided in vivo evidence that the posteromedial cortices are among the earliest sites of amyloid β ($A\beta$) plaque accumulation—one of the pathologic hallmarks of AD.^{28,29} Interestingly, *APOE* $\epsilon 4$ is known to increase brain's vulnerability to $A\beta$ pathology,^{30,31} and even before the formation of $A\beta$ plaques, to induce neurotoxicity of soluble $A\beta$ oligomers.³²⁻³⁴ Both the increased $A\beta$ plaque deposition and impaired synaptic transmission due to $A\beta$ oligomers in $\epsilon 4$ carriers provide potential biologic mechanisms for the posteromedial cortical dysfunction observed in this fMRI study. It remains unknown that how amyloid pathology

results in decreased resting glucose metabolism as observed with PET and inability to effectively modulate the neuronal activity in these posteromedial cortical regions as demonstrated with fMRI. It may be that regions which show evidence of decreased metabolism at rest are unable to respond to further decrease in activity during goal-directed task performance to support, for example, memory encoding.^{35,36} Given the strong interconnectivity between the posteromedial and medial temporal cortices,³⁷ it is also possible that impaired posteromedial cortical function in the $\epsilon 4$ carriers versus noncarriers reflects remote effects of more pronounced neurofibrillary tangle pathology in the medial temporal regions of the $\epsilon 4$ carriers.^{28,31,38,39}

The same posteromedial regions vulnerable to hypometabolism during rest and impaired fMRI response pattern during goal-directed cognitive tasks have been proposed as key components of the default network⁴⁰ and of large-scale memory networks.⁴¹ The cognitive operations supported by the posteromedial cortices are, however, not fully understood. In young subjects, the default network regions typically show deactivation during most goal-oriented cognitive tasks, however, new fMRI studies suggest that the posteromedial cortices may have a specific role in memory formation and retrieval. There is recent fMRI evidence that deactivation of the posteromedial cortices during encoding supports successful memory formation,^{35,36} and that the same posteromedial cortices which are deactivated during successful encoding, are activated during memory retrieval.⁴² Furthermore, fMRI studies suggest that retrieval-related activity of these regions is impaired in MCI.⁴³ Our current study is in agreement with the hypothesis that greater fMRI deactivation during encoding is related to better memory ability, even when measured via delayed recall as in standard neuropsychologic tests, both within cognitively intact older individuals and across a spectrum of clinical impairment. Interestingly, both right and left posteromedial cortical activity was significantly compromised in the $\epsilon 4$ carriers but only magnitude of the left posteromedial fMRI signal correlated with verbal memory measures.

In this study, upregulation of the posteromedial cortical fMRI activity in subjects at risk for AD was observed in the context of a widespread network of brain

areas demonstrating increased fMRI activity in $\epsilon 4$ carriers compared with noncarriers. Among these regions, similar to posteromedial cortices, the ventral anterior cingulum is often considered as part of the default network, and typically demonstrates deactivation during externally directed cognitive tasks, such as intentional encoding.^{40,41} Other regions which showed increased fMRI activity in $\epsilon 4$ carriers, however, are parts of attentional and working memory networks, which typically activate during demanding memory tasks. Similar to our study, increased lateral prefrontal activity in $\epsilon 4$ carriers has been reported in previous fMRI studies^{44,45} and has been interpreted to be compensatory in nature.⁴⁶ It is also possible that early AD pathology, more likely to be present in the $\epsilon 4$ carriers, is associated with widespread cortical irritability or chronic upregulation of neuronal activity.⁴⁷

Our study has several limitations, which need to be addressed in future studies. We analyzed fMRI data from elderly subjects spanning a wide cognitive range and stratified by the *APOE* $\epsilon 4$ allele status. There were, however, relatively small numbers of $\epsilon 4$ carriers within each clinical subgroup. We did not have detailed data available on the family history of AD for all of the subjects. Recent fMRI studies have interestingly suggested complex interactions between cognitive performance, *APOE* genotype and family history effects on fMRI activity.^{48,49} In this study, we did not perform a whole-brain structural voxel-based morphometric analysis between the study groups, although we did use the gray matter volumes as covariates in the functional data analyses. It is worth noting that the task-related BOLD fMRI is always a relative measure investigating the net difference between 2 cognitive conditions, that is, there is not a quantitative zero baseline from which BOLD signal would vary up or down.^{50,51} It is also possible that some of the observed differences between groups were due to different cognitive strategies, that is the nature of the encoding task may have been more challenging or emotionally taxing to the subjects who have dementia or are concerned that they may have a memory problem. Patients with greater cognitive impairment may also be in a different cognitive state during the fixation baseline condition, which is also an issue in resting functional connectivity MRI studies. Nevertheless, we observed consistent alterations in posteromedial cortical activity related to both the presence of the $\epsilon 4$ allele and performance on an episodic memory task, even among clinically normal subjects. Further clinical follow-up will be necessary to determine if these healthy older subjects will progress to demonstrate cognitive impairment and eventual clinical dementia. Finally, there may be alterations in BOLD fMRI activity that are related to neurovascular coupling or vascular factors.^{52–54} Future studies may incorporate arterial spin labeling or gadolinium dynamic contrast perfusion MRI techniques to determine whether, for example, regional alterations in the baseline blood flow are responsible for some of the observed relative differences between $\epsilon 4$ carriers and noncarriers.

In conclusion, our findings suggest that abnormal fMRI response pattern in the posteromedial cortices may be an early indicator of brain dysfunction and is related to risk factors for developing AD. Functional imaging of the posteromedial cortices may provide a sensitive technique to track alterations in neural activity due to evolving AD pathology, identify subjects at risk for developing AD, and potentially monitor response to disease-modifying therapy.

ACKNOWLEDGMENTS

The authors thank the staff of the Massachusetts General Hospital Gerontology Research Unit and Brigham and Women's Hospital Memory Disorders Unit Clinical Research for assistance with subject recruitment, evaluation, and data management, as well as Mary Foley, Larry White, and the Athinoula A. Martinos Center staff for assistance with MRI data collection. They also thank Kristina DePeau, Elizabeth Chua, Saul Miller, Kim Celone, and Eli Diamond for assistance with data collection and analyses. They express special gratitude to the subjects who participated in this study.

REFERENCES

- Lustig C, Snyder AZ, Bhakta M, et al. Functional deactivations: change with age and dementia of the Alzheimer type. *Proc Natl Acad Sci U S A*. 2003;100:14504–14509.
- Greicius MD, Srivastava G, Reiss AL, et al. Default-mode network activity distinguishes Alzheimer's disease from healthy aging: evidence from functional MRI. *Proc Natl Acad Sci U S A*. 2004;101:4637–4642.
- Rombouts SA, Barkhof F, Goekoop R, et al. Altered resting state networks in mild cognitive impairment and mild Alzheimer's disease: an fMRI study. *Hum Brain Mapp*. 2005;26:231–239.
- Petrella JR, Wang L, Krishnan S, et al. Cortical deactivation in mild cognitive impairment: high-field-strength functional MR imaging. *Radiology*. 2007;245:224–235.
- Sorg C, Riedl V, Muhlau M, et al. Selective changes of resting-state networks in individuals at risk for Alzheimer's disease. *Proc Natl Acad Sci U S A*. 2007;104:18760–18765.
- Zhou Y, Dougherty JH Jr, Hubner KF, et al. Abnormal connectivity in the posterior cingulate and hippocampus in early Alzheimer's disease and mild cognitive impairment. *Alzheimers Dement*. 2008;4:265–270.
- Hämäläinen A, Tervo S, Grau-Olivares M, et al. Voxel-based morphometry to detect brain atrophy in progressive mild cognitive impairment. *Neuroimage*. 2007;37:1122–1131.
- Whitwell JL, Shiung MM, Przybelski SA, et al. MRI patterns of atrophy associated with progression to AD in amnesic mild cognitive impairment. *Neurology*. 2008;70:512–520.
- Saunders AM, Strittmatter WJ, Schmechel D, et al. Association of apolipoprotein E allele epsilon 4 with late-onset familial and sporadic Alzheimer's disease. *Neurology*. 1993;43:1467–1472.
- Bertram L, McQueen MB, Mullin K, et al. Systematic meta-analyses of Alzheimer disease genetic association studies: the AlzGene database. *Nat Genet*. 2007;39:17–23.
- Reiman EM, Caselli RJ, Yun LS, et al. Preclinical evidence of Alzheimer's disease in persons homozygous for the epsilon 4 allele for apolipoprotein E. *N Engl J Med*. 1996;334:752–758.
- Small GW, Mazziotta JC, Collins MT, et al. Apolipoprotein E type 4 allele and cerebral glucose metabolism in relatives at risk for familial Alzheimer disease. *JAMA*. 1995;273:942–947.
- Rapoport SI. Positron emission tomography in Alzheimer's disease in relation to disease pathogenesis: a critical review. *Cerebrovasc Brain Metab Rev*. 1991;3:297–335.
- Minoshima S, Giordani B, Berent S, et al. Metabolic reduction in the posterior cingulate cortex in very early Alzheimer's disease. *Ann Neurol*. 1997;42:85–94.
- Herholz K, Salmon E, Perani D, et al. Discrimination between Alzheimer dementia and controls by automated analysis of multicenter FDG PET. *Neuroimage*. 2002;17:302–316.
- Nestor PJ, Fryer TD, Smielewski P, et al. Limbic hypometabolism in Alzheimer's disease and mild cognitive impairment. *Ann Neurol*. 2003;54:343–351.
- Morris JC. Clinical dementia rating: a reliable and valid diagnostic and staging measure for dementia of the Alzheimer type. *Int Psychogeriatr*. 1997;9(suppl 1):173–176.

18. McKhann G, Drachman D, Folstein M, et al. Clinical diagnosis of Alzheimer's disease: report of the NINCDS-ADRDA Work Group under the auspices of Department of Health and Human Services Task Force on Alzheimer's Disease. *Neurology*. 1984;34:939–944.
19. Dickerson BC, Salat DH, Greve DN, et al. Increased hippocampal activation in mild cognitive impairment compared to normal aging and AD. *Neurology*. 2005;65:404–411.
20. Celone KA, Calhoun VD, Dickerson BC, et al. Alterations in memory networks in mild cognitive impairment and Alzheimer's disease: an independent component analysis. *J Neurosci*. 2006;26:10222–10231.
21. Dickerson BC, Sperling RA, Hyman BT, et al. Clinical prediction of Alzheimer disease dementia across the spectrum of mild cognitive impairment. *Arch Gen Psychiatry*. 2007;64:1443–1450.
22. Hixson JE, Vernier DT. Restriction isotyping of human apolipoprotein E by gene amplification and cleavage with HhaI. *J Lipid Res*. 1990;31:545–548.
23. Sperling RA, Bates JF, Cocchiarella AJ, et al. Encoding novel face-name associations: a functional MRI study. *Hum Brain Mapp*. 2001;14:129–139.
24. Smith SM, Zhang Y, Jenkinson M, et al. Accurate, robust, and automated longitudinal and cross-sectional brain change analysis. *Neuroimage*. 2002;17:479–489.
25. Beckmann CF, Jenkinson M, Smith SM. General multilevel linear modeling for group analysis in fMRI. *Neuroimage*. 2003;20:1052–1063.
26. Worsley KJ, Evans AC, Marrett S, et al. A three-dimensional statistical analysis for CBF activation studies in human brain. *J Cereb Blood Flow Metab*. 1992;12:900–918.
27. Persson J, Lind J, Larsson A, et al. Altered deactivation in individuals with genetic risk for Alzheimer's disease. *Neuropsychologia*. 2008;46:1679–1687.
28. Braak H, Braak E. Neuropathological staging of Alzheimer-related changes. *Acta Neuropathol (Berl)*. 1991;82:239–259.
29. Mintun MA, Larossa GN, Sheline YI, et al. [11C]PIB in a nondemented population: potential antecedent marker of Alzheimer disease. *Neurology*. 2006;67:446–452.
30. Schmechel DE, Saunders AM, Strittmatter WJ, et al. Increased amyloid beta-peptide deposition in cerebral cortex as a consequence of apolipoprotein E genotype in late-onset Alzheimer disease. *Proc Natl Acad Sci U S A*. 1993;90:9649–9653.
31. Ohm TG, Kirca M, Bohl J, et al. Apolipoprotein E polymorphism influences not only cerebral senile plaque load but also Alzheimer-type neurofibrillary tangle formation. *Neuroscience*. 1995;66:583–587.
32. Selkoe DJ. Alzheimer's disease is a synaptic failure. *Science*. 2002;298:789–791.
33. Tanzi RE. The synaptic Abeta hypothesis of Alzheimer disease. *Nat Neurosci*. 2005;8:977–979.
34. Manelli AM, Bulfinch LC, Sullivan PM, et al. Abeta42 neurotoxicity in primary co-cultures: effect of apoE isoform and Abeta conformation. *Neurobiol Aging*. 2007;28:1139–1147.
35. Daselaar SM, Prince SE, Cabeza R. When less means more: deactivations during encoding that predict subsequent memory. *Neuroimage*. 2004;23:921–927.
36. Miller SL, Celone K, Depeau K, et al. Age-related memory impairment associated with loss of parietal deactivation but preserved hippocampal activation. *Proc Natl Acad Sci U S A*. 2008;105:2181–2186.
37. Kobayashi Y, Amaral DG. Macaque monkey retrosplenial cortex: III. Cortical efferents. *J Comp Neurol*. 2007;502:810–833.
38. Meguro K, Blaizot X, Kondoh Y, et al. Neocortical and hippocampal glucose hypometabolism following neurotoxic lesions of the entorhinal and perirhinal cortices in the non-human primate as shown by PET. Implications for Alzheimer's disease. *Brain*. 1999;122:1519–1531.
39. Bradley KM, O'Sullivan VT, Soper ND, et al. Cerebral perfusion SPET correlated with Braak pathological stage in Alzheimer's disease. *Brain*. 2002;125:1772–1781.
40. Raichle ME, MacLeod AM, Snyder AZ, et al. A default mode of brain function. *Proc Natl Acad Sci U S A*. 2001;98:676–682.
41. Buckner RL, Snyder AZ, Shannon BJ, et al. Molecular, structural, and functional characterization of Alzheimer's disease: evidence for a relationship between default activity, amyloid, and memory. *J Neurosci*. 2005;25:7709–7717.
42. Shannon BJ, Buckner RL. Functional-anatomic correlates of memory retrieval that suggest nontraditional processing roles for multiple distinct regions within posterior parietal cortex. *J Neurosci*. 2004;24:10084–10092.
43. Johnson SC, Schmitz TW, Moritz CH, et al. Activation of brain regions vulnerable to Alzheimer's disease: the effect of mild cognitive impairment. *Neurobiol Aging*. 2006;27:1604–1612.
44. Bookheimer SY, Strojwas MH, Cohen MS, et al. Patterns of brain activation in people at risk for Alzheimer's disease. *N Engl J Med*. 2000;343:450–456.
45. Han SD, Houston WS, Jak AJ, et al. Verbal paired-associate learning by APOE genotype in non-demented older adults: fMRI evidence of a right hemispheric compensatory response. *Neurobiol Aging*. 2007;28:238–247.
46. Zarahn E, Rakitin B, Abela D, et al. Age-related changes in brain activation during a delayed item recognition task. *Neurobiol Aging*. 2007;28:784–798.
47. Busche MA, Eichhoff G, Adelsberger H, et al. Clusters of hyperactive neurons near amyloid plaques in a mouse model of Alzheimer's disease. *Science*. 2008;321:1686–1689.
48. Johnson SC, Schmitz TW, Trivedi MA, et al. The influence of Alzheimer disease family history and apolipoprotein E epsilon4 on mesial temporal lobe activation. *J Neurosci*. 2006;26:6069–6076.
49. Xu G, McLaren DG, Ries ML, et al. The influence of parental history of Alzheimer's disease and apolipoprotein E epsilon4 on the BOLD signal during recognition memory. *Brain*. 2009;132:383–391.
50. Stark CE, Squire LR. When zero is not zero: the problem of ambiguous baseline conditions in fMRI. *Proc Natl Acad Sci U S A*. 2001;98:12760–12766.
51. Morcom AM, Fletcher PC. Does the brain have a baseline? Why we should be resisting a rest. *Neuroimage*. 2007;37:1073–1082.
52. D'Esposito M, Deouell LY, Gazzaley A. Alterations in the BOLD fMRI signal with ageing and disease: a challenge for neuroimaging. *Nat Rev Neurosci*. 2003;4:863–872.
53. Johnson NA, Jahng GH, Weiner MW, et al. Pattern of cerebral hypoperfusion in Alzheimer disease and mild cognitive impairment measured with arterial spin-labeling MR imaging: initial experience. *Radiology*. 2005;234:851–859.
54. Luckhaus C, Flub MO, Wittsack HJ, et al. Detection of changed regional cerebral blood flow in mild cognitive impairment and early Alzheimer's dementia by perfusion-weighted magnetic resonance imaging. *Neuroimage*. 2008;40:495–503.